

# FCC-ee DYNAMIC APERTURE STUDIES AND FREQUENCY MAP ANALYSIS

T. Tydecks\*, S. Aumon, T. K. Charles, B. Haerer, B. Holzer,  
 K. Oide, Y. Papaphilippou, J. Wenninger, CERN, Geneva, Switzerland

## Abstract

The FCC-ee Lepton Collider will provide  $e^+e^-$  collisions in the beam energy range of 45.6 GeV to 182.5 GeV. FCC-ee will be a precision measurement tool for  $Z$ ,  $W$ ,  $H$  and  $t$  physics with expected luminosities of  $2.07 \times 10^{36} \text{ cm}^{-2} \text{ s}^{-1}$  at the  $Z$ -pole and  $1.3 \times 10^{34} \text{ cm}^{-2} \text{ s}^{-1}$  at the  $t\bar{t}$  threshold. In order to achieve the foreseen luminosities, a vertical  $\beta^*$  of 1 mm to 2 mm is mandatory. Dynamic aperture and frequency map analysis for the 97.75-km machine with such a squeezed accelerator optics are studied. Furthermore, effects of machine misalignments on dynamic and momentum aperture are presented and estimations for the required tolerances are given.

## INTRODUCTION

FCC-ee will be a precision measurement tool for  $Z$ ,  $W$ ,  $H$ , and  $t\bar{t}$ , yielding unprecedented luminosities [1]. To achieve this goal, it is mandatory to push  $\beta^*$  to the milli-meter scale in the vertical plane. Furthermore, continuous top-up injection is necessary to guarantee high luminosities. Therefore, injection into a fully squeezed machine optics must be possible. A lossless injection is guaranteed if sufficient dynamic aperture and momentum aperture are present.

Dynamic aperture is governed by nonlinear beam dynamics being caused by the introduction of higher order multipoles like sextupoles in the lattice as well as machine imperfections like misalignments and multipole errors. With small beam size arises the necessity to have strong sextupole fields in order to correct the large natural beam chromaticities, necessary to achieve sufficient momentum aperture. Strong sextupoles in turn affect tune shift with amplitude, reducing dynamic aperture. The sextupole lattice for FCC-ee is made of pairs of identical sextupoles placed in a distance corresponding to  $180^\circ$  phase advance. Thus, geometric aberrations are canceled and tune shift with amplitude is reduced.

Dynamic and momentum aperture are studied by means of particle tracking. Tracking was done using MAD-X-PTC [2, 3]. All studies were performed for a beam energy of 175 GeV.

## DYNAMIC APERTURE WITHOUT ERRORS

The machine without misalignments was tested by tracking particles for 2000 turns on an equally spaced grid in  $x$  and  $y$  (comp. Fig. 1). Tracking was done in 4D, i. e. no radiation effects or synchrotron motion was taken into account.

\* tobias.tydecks@cern.ch

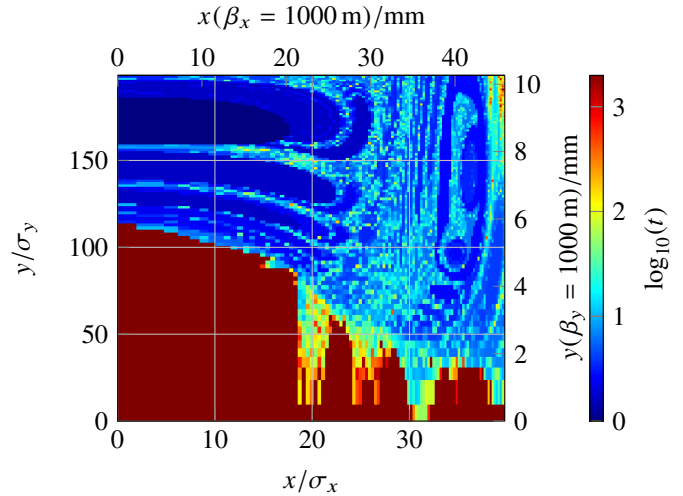


Figure 1: Logarithm of number of survived turns in color code as function of transverse initial amplitudes.

Figure 1 shows that the region of stability appears to be limited to  $\sim 20 \sigma_x$  and  $\sim 110 \sigma_y$  in the horizontal and vertical plane, respectively. The corresponding amplitudes in real space for an arbitrary value for the corresponding  $\beta$ -function of 1000 m are presented as secondary  $x/y$ -axis in Fig. 1. The apparently stable island-like structures for higher horizontal amplitudes require the particles to jump over the integer resonance and will disappear once radiation effects are taken into account and misalignments are introduced.

## Frequency Map Analysis

In order to study the non-linear beam dynamics of the machine, we now focus on the previously determined stable region between zero and  $20 \sigma_x$  horizontally and zero and  $100 \sigma_y$  vertically.

Frequency map analysis (FMA) [4] is applied to study the non-linear beam dynamics in order to identify harmful resonances. The diffusion rate is defined as

$$d = \log_{10} \left[ \sqrt{\left( \nu_x^{(2)} - \nu_x^{(1)} \right)^2 + \left( \nu_y^{(2)} - \nu_y^{(1)} \right)^2} \right], \quad (1)$$

where  $\nu_i^{(1)}$  and  $\nu_i^{(2)}$  refer to the tune determined from the 1<sup>st</sup> and 2<sup>nd</sup> half of the tracked turns using numerical analysis of fundamental frequencies (NAFF) [5].

Tracking was done for 2000 turns without radiation effects. In Fig. 2, the diffusion is displayed in color code as a function of both amplitude and corresponding tune (determined from the complete 2000 turns).

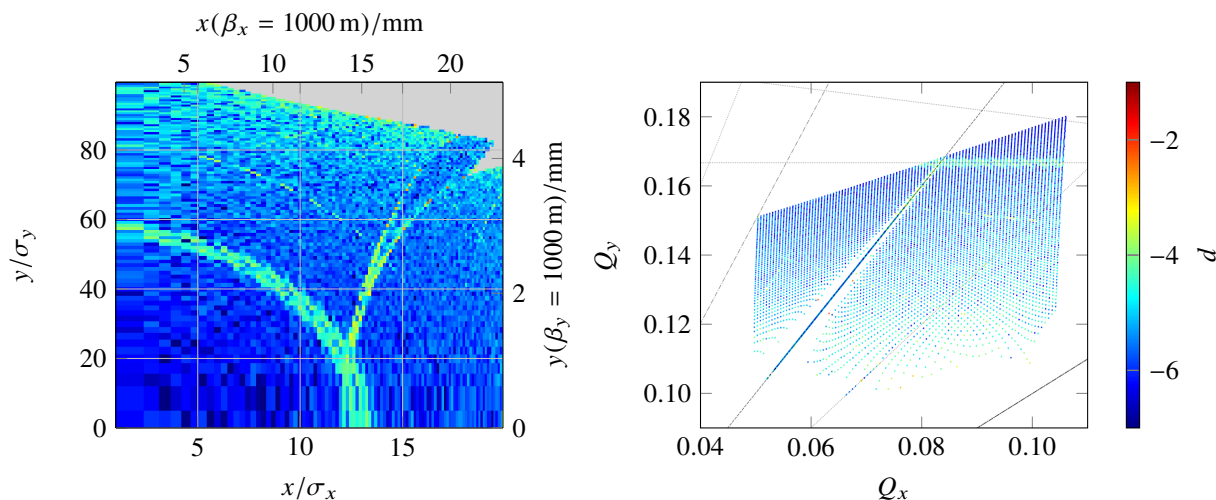


Figure 2: Diffusion  $d$  inside transverse dynamic aperture (left) and as a function of tune (right).

From the diffusion, we can observe that the two dominant resonances interacting with the beam within the studied aperture are the following:

- The first one corresponds to  $Q_y = 1/6$ , seen in the dynamic aperture as a circle around the origin and touching the  $y$ -axis at  $\sim 55 \sigma_y$ .
- The second one is the coupling resonance  $Q_y = 2Q_x$ , seen in the dynamic aperture as a hook touching the  $x$ -axis at  $\sim 12$  to  $13 \sigma_x$ .

Since misalignments tend to drive resonances, we can expect that the dynamic aperture including misalignment errors will be limited to 12 to 13  $\sigma_x$  horizontally and 55  $\sigma_y$  vertically, corresponding to  $x_0 = 0.43$  mm and  $y_0 = 3.9 \mu\text{m}$  at the interaction point (IP), for  $\beta_x^* = 1$  m and  $\beta_y^* = 2$  mm, and for emittances  $\varepsilon_x = 1.3$  nm rad and  $\varepsilon_y = 2.5$  pm rad.

## MISALIGNMENTS

To study more realistic machines, misalignments have to be introduced and corrected for. A procedure was established for correcting misalignments [6].

The misalignment amplitudes used for this study are presented in Tab. 1. Errors were assigned with a Gaussian random number generator truncated at  $2.5 \sigma$ . The corrections were performed at 1 GeV beam energy to avoid perturbations by energy sawtooth.

After applying a correction scheme to the misaligned lattice, the energy was increased to 175 GeV and the machine was tapered, i. e. the strength of each element was adjusted

Table 1: Misalignment Errors used for this Study

	$\sigma_x$	$\sigma_y$	$\sigma_\theta$
arc quadrupoles	100 $\mu\text{m}$	100 $\mu\text{m}$	100 $\mu\text{rad}$
IP quadrupoles	50 $\mu\text{m}$	50 $\mu\text{m}$	50 $\mu\text{rad}$
sextupoles	100 $\mu\text{m}$	100 $\mu\text{m}$	

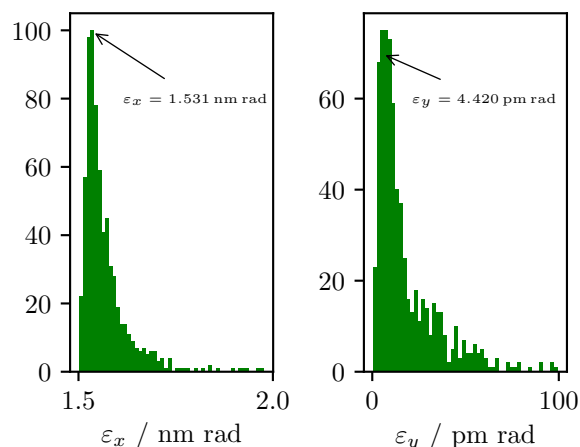


Figure 3: Distribution of horizontal and vertical emittance after correction for 690 error seeds which converged out of 1000 error seeds.

according to the local beam energy. Using the EMIT module in MAD-X, the emittance was determined. The resulting emittances after tapering at 175 GeV are displayed in Fig. 3.

Out of 1000 seeds, 690 seeds converged, meaning that the final EMIT command yielded a horizontal emittance smaller than 3.0 nm rad and a vertical emittance smaller than 100 pm rad.

## DYNAMIC APERTURE WITH MISALIGNMENTS

For the corrected machines which converged, the dynamic aperture was determined by tracking particles with increasing amplitude and determining the threshold for particle losses. First a coarse scan is performed to estimate the aperture, afterwards a fine scan is performed yielding a final accuracy of 2.5  $\mu\text{m}$  in the horizontal plane and 25 nm in the vertical plane.

Content from this work may be used under the terms of the CC BY 3.0 licence (© 2018). Any distribution of this work must maintain attribution to the author(s), title of the work, publisher, and DOI.

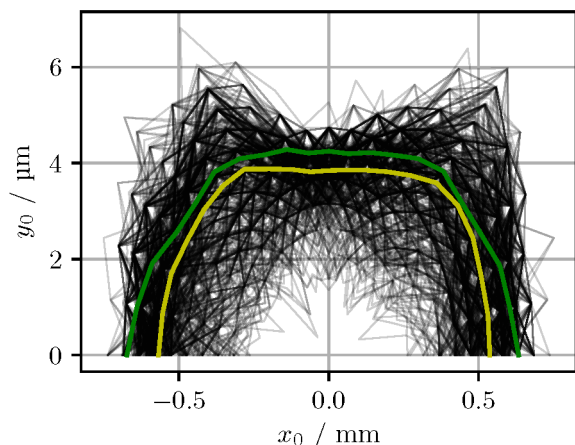


Figure 4: Dynamic aperture with (grey) and without (green) misalignment errors including radiation damping and quantum excitation for 675 out of 1000 seeds. Average for seeds indicated in yellow.

Tracking was done for 100 turns, which corresponds to  $\sim 4$  longitudinal damping times including radiation damping and quantum excitation.

The resulting aperture for converged error seeds is shown in Fig. 4. Out of 690 converged seeds, 675 yield a horizontal aperture larger than  $\pm 0.25$  mm at the IP (corresponding to an aperture larger than  $6\sigma_x$ ). In the vertical plane, we observe a large spread in aperture. This is due to the fact that the distribution of vertical emittance shows a rather large spread with a long tail (comp. Fig. 3).

The average horizontal aperture is limited to  $-0.57$  mm /  $0.54$  mm, corresponding to  $14.4\sigma_x$  /  $13.6\sigma_x$  assuming  $1.531$  nm rad for the horizontal emittance, which is the peak value found in Fig. 3.

The results for average horizontal aperture fit well to our estimations from FMA.

## MOMENTUM APERTURE WITH MISALIGNMENTS

For operation and injection, the momentum aperture has to be sufficiently large as well. The momentum aperture for the converged error seeds is displayed in Fig. 5. Out of 690 converged seeds, 675 seeds yield a horizontal on-momentum aperture larger than  $0.25$  mm at the IP. The average momentum aperture appears to be  $-2.5\%$  /  $+2.1\%$ .

## CONCLUSION

Introducing realistic misalignments / roll angles to the machine reduces both dynamic and momentum aperture. After filtering for emittance and usable dynamic and momentum aperture, 675 out of 1000 error seeds are left.

Frequency map analysis provides hints to possible measures to increase the dynamic aperture: lowering the vertical tune below the  $Q_y = 1/6$  resonance and simultaneously increasing the horizontal distance to the  $Q_y = 2Q_x$  resonance could possibly improve the dynamic aperture and shall be

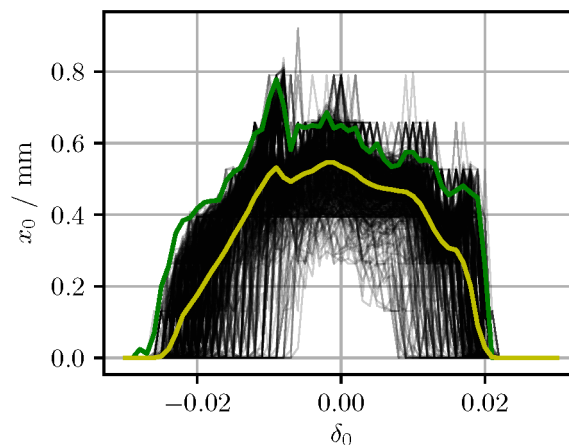


Figure 5: Momentum aperture with (grey) and without (green) misalignment errors including radiation damping and quantum excitation for 675 out of 1000 seeds. Average for seeds indicated in yellow.

studied. Furthermore, dynamic aperture may be increased by additional (skew) sextupole optimization. The momentum aperture appears to be large enough to store beam and provides sufficient aperture for longitudinal injection.

For the next steps in this study, different misalignment amplitudes as well as field and gradient errors will be studied in order to determine the requirements and limitations for the injection scheme. Furthermore, additional correction steps need to be included at 175 GeV beam energy to reduce residual emittance coupling at high energy.

## ACKNOWLEDGEMENT

The authors would like to thank the management of CERN for supporting this work as well as Piotr Skowronski for excellent MAD-X-PTC support and Frank Zimmermann for fruitful discussion.

## REFERENCES

- [1] J. Wenninger *et al.*, "Future circular collider study lepton collider parameters," CERN Report FCC-1401201640-DSC, Geneva, Switzerland, 2016.
- [2] L. Deniau *et al.*, "The MADX program (Methodical Accelerator Design) version 5.03.07 user's reference manual," CERN Internal Document, Geneva, Switzerland, 2017.
- [3] E. Forest *et al.*, "Introduction to the polymorphic tracking code," CERN Report CERN-SL-2002-044, 2002.
- [4] Y. Papaphilippou, "Detecting chaos in particle accelerators through frequency map analysis method," Chaos 24 p. 024412, 2014.
- [5] J. Laskar, "The chaotic motion of the solar system. A numerical estimate of the size of the chaotic zones," Icarus, 88, p. 266-291, 1990.
- [6] S. Aumon *et al.*, "Tolerance studies and dispersion free steering for extreme low emittance in the FCC-ee project," in *Proc. of IPAC2016*, pp. 3759-3762, Busan, Korea, 2016.